

Shock model description of the interaction radiation pulse in nested wire array z-pinch

D. J. Ampleford, C. A. Jennings, S. V. Lebedev, S. N. Bland, M. E. Cuneo, D. B. Sinars, S. C. Bott, G. N. Hall, F. Suzuki-Vidal, J. B. A. Palmer, and J. P. Chittenden

Citation: *Physics of Plasmas* **19**, 122711 (2012); doi: 10.1063/1.4771673

View online: <http://dx.doi.org/10.1063/1.4771673>

View Table of Contents: <http://scitation.aip.org/content/aip/journal/pop/19/12?ver=pdfcov>

Published by the [AIP Publishing](#)

Articles you may be interested in

[Two-dimensional magnetohydrodynamic studies of implosion modes of nested wire array z-pinch](#)

Phys. Plasmas **21**, 072707 (2014); 10.1063/1.4890474

[Effective versus ion thermal temperatures in the Weizmann Ne Z-pinch: Modeling and stagnation physics](#)

Phys. Plasmas **21**, 031209 (2014); 10.1063/1.4865223

[Shock waves in a Z-pinch and the formation of high energy density plasma](#)

Phys. Plasmas **19**, 122701 (2012); 10.1063/1.4769264

[Dynamics of conical wire array Z-pinch implosions](#)

Phys. Plasmas **14**, 102704 (2007); 10.1063/1.2795129

[Amplitude reduction of nonuniformities induced by magnetic Rayleigh–Taylor instabilities in Z-pinch dynamic hohlraums](#)

Phys. Plasmas **12**, 012703 (2005); 10.1063/1.1819936



PFEIFFER VACUUM

VACUUM SOLUTIONS FROM A SINGLE SOURCE

Pfeiffer Vacuum stands for innovative and custom vacuum solutions worldwide, technological perfection, competent advice and reliable service.

125 YEARS NOTHING IS BETTER

Shock model description of the interaction radiation pulse in nested wire array z-pinch

D. J. Ampleford,^{1,a)} C. A. Jennings,¹ S. V. Lebedev,² S. N. Bland,² M. E. Cuneo,¹
 D. B. Sinars,¹ S. C. Bott,³ G. N. Hall,² F. Suzuki-Vidal,² J. B. A. Palmer,²
 and J. P. Chittenden²

¹Sandia National Laboratories, Albuquerque, New Mexico 87185-1106, USA

²The Blackett Laboratory, Imperial College, London SW7 2BW, United Kingdom

³Center for Energy Research, University of California, San Diego, La Jolla, CA 92093, USA

(Received 18 July 2012; accepted 9 November 2012; published online 27 December 2012)

Bow shock structures are observed in a nested wire array z-pinch as ablation streams from the outer array pass the inner array. The jump in plasma conditions across these shocks results in an enhancement of snowplow emission from the imploding plasma piston. Results from a snowplow model modified to account for the shock jumps are discussed and compared to experimental data from MAGPIE. Magnetohydrodynamic simulations indicate that this is the primary heating mechanism responsible for the interaction pulse recorded on the Z generator, which is required for pulse shaping for inertial confinement fusion. © 2012 American Institute of Physics.
[\[http://dx.doi.org/10.1063/1.4771673\]](http://dx.doi.org/10.1063/1.4771673)

I. BACKGROUND

Nested wire array z-pinch¹ have previously been proposed as a potential driver for indirect inertial confinement fusion (ICF).² The interaction pulse, which is emitted as the outer array of a nested wire array reaches the inner array, plays a critical role in creating the pulse shape required for ICF.^{3,4} The mechanisms responsible for this x-ray pulse are not, however, well understood.⁵ Early assumptions of a hydrodynamic collision of the outer and inner shells have been disproved by the observed transparency of the inner array^{6–9} and the insensitivity of the emitted power pulse to different inner array setups (e.g., inner wire number⁵).

In this paper, we propose a new mechanism which could be responsible for the interaction pulse in nested wire arrays operating in transparent mode. Our experimental data obtained on the IMA MAGPIE facility show that precursor plasma flowing from the outer array forms a system of standing bow shocks at the inner array wires. Previous work has considered the role of bow shocks created in the imploding outer material due to the inner wire array, however here, for the first time, we consider the effect that these bow shocks formed in the ablation streams from the outer array have on the final implosion. These discontinuities increase the density and decrease the velocity of the plasma prefill. Inelastic accretion of this perturbed material by the imploding piston leads to an increase of the snowplow radiation above the level observed in the single wire arrays and produces the interaction x-ray pulse. Previously, similar shocks in nested wire arrays were explored as a test-bed for studies of astrophysical bow shocks.¹¹

Experiments were performed on the MAGPIE generator using nested Al wire arrays with $32 \times 10 \mu\text{m}$ wires in the outer array at a diameter of 16 mm and $16 \times 15 \mu\text{m}$ wires in the inner array at a diameter of 8 mm. In nested wire arrays

on the Z-generator, the high wire number in the outer array leads to a minimal current through the inner array. To recreate a similar current fraction through the inner array on MAGPIE, the inductance of the inner array is enhanced by geometry; for experiments on MAGPIE an inner array 3.6 times the length of the outer array is used, as described by Refs. 7 and 9. The MAGPIE experiments described here use a wire array setup identical to that used by Bland *et al.*⁹ Figure 1 shows the difference in nested wire array setups for Z and for MAGPIE.

For experiments on MAGPIE, the main diagnostics that we will use in the discussion here are Extreme-UV (XUV) self-emission imaging and streak photography. Two XUV imaging systems¹⁰ are used, one looking radially, or side-on, to the array and one looking end-on down the axis of symmetry of the array (in reality this camera was positioned a few degrees off-axis). These each use an un-filtered pinhole to image onto a Micro-Channel Plate; diffraction at the pinhole providing a 30 eV lower limit to the photon energies imaged.¹⁰ The streak camera is used to image a radial chord across the center of the pinch as a function of time. A narrow slit limits the axial extent imaged onto the camera to $\sim 100 \mu\text{m}$.

II. OBSERVATION OF SHOCKS ON MAGPIE

Wire array z-pinchs are now understood to not implode as a uniform (0-dimensional) plasma shell.^{5,7,12–14} Instead the wires undergo a steady ablation of material toward the array axis. For nested wire arrays, the outer array undergoes this ablation in a similar manner to an identical single array. This wire ablation can be well characterized by a rocket model where, for a given setup, the velocity of ablated material is taken to be fixed.¹² After a substantial depletion of material from the wire cores ($\sim 50\%$), the outer (or single) array begins to implode, with the imploding piston accreting the prefill material (commonly referred to as the snowplow). Excess power from the inelastic accretion of the prefill

^{a)}Electronic address: damplef@sandia.gov.

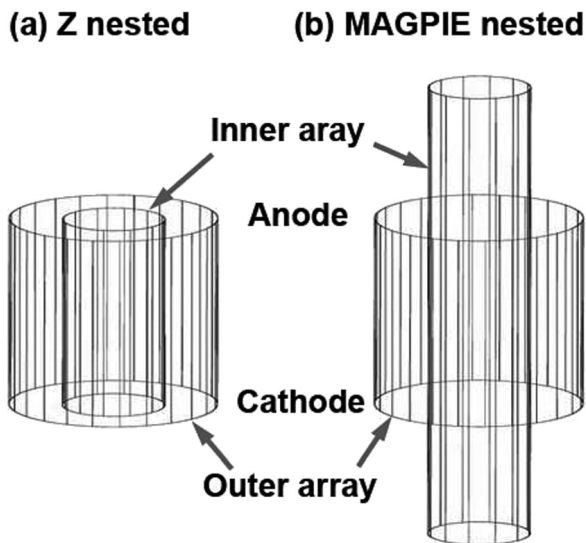


FIG. 1. Nested wire array setups for (a) Z and (b) MAGPIE showing the difference in relative length of the inner array used to control the inner array current fraction.

material by the piston is radiated as snowplow emission (on a timescale much shorter than the characteristic timescales of the system). The power emitted by the snowplow (P_{SP}) is determined by energy balance, $P_{SP} = \rho(\Delta v)^3$, where ρ is the density and Δv is the velocity difference between the imploding plasma and the prefill material. For a nested wire array, as the imploding outer passes the inner array, current is switched into the inner. It is at this time that the interaction pulse is emitted (prior to the implosion of the inner array). Previous analysis has assumed that the snowplow emission switches off as current is switched out of the outer array, and it coasts current free toward the axis. Here, we explore how the presence of the inner array wires alters the ablated plasma flows that are then accreted by the snowplow piston and, in turn, what effect this modified prefill has on the snowplow emission.

The precursor plasma streams in wire array z-pinchs are highly supersonic (Mach number $M = v_{abl}/c_s \sim 5$ for Al arrays on MAGPIE,¹⁵ and $M > 11.5$ for W arrays on Z (Ref. 5)). For a nested wire array, the inner array acts as an obstruction to these supersonic flows, resulting in the formation of shocks.

Figure 2 shows end-on self-emission imaging ($h\nu > 30$ eV) of the region near the location of the inner array prior to start of the outer array implosion on MAGPIE. Bow shock structures are present around each of the inner wires, as drawn on the diagram in the figure. These bow shocks are created as the supersonic incoming flow is perturbed by the presence of the inner wire cores, which are 15–25 μm in diameter. Previous experiments with an identical setup⁹ have demonstrated that there is < 1 kA current through the inner array wires at this time, hence the pressure due to the magnetic field produced by current through the inner array wires will have a negligible effect with respect to the ram pressure both upstream and downstream of the shock.

For this setup the angle of these shocks to the direction of the ablation flows is measured as $\beta \sim 40^\circ$, and appears

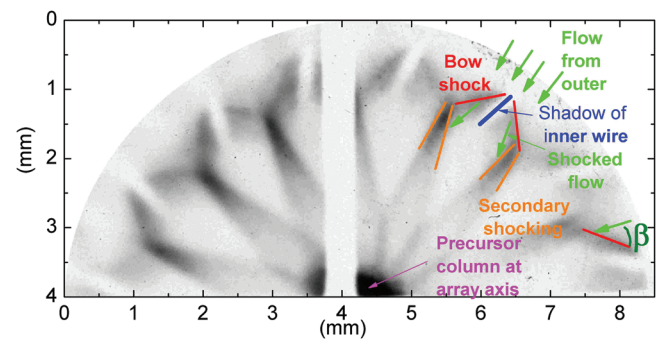


FIG. 2. End-on self emission imaging ($h\nu > 30$ eV; set by diffraction) at 201–211 ns demonstrates that bow shocks are present in the flow around the wires of the inner array (the inner array diameter is 8 mm). The image is before the start of the implosion phase of the outer. Labels show the interpretation of this structure as discussed in the text.

static in time (over ≥ 30 ns). There is a small curvature to the shock, however for the present discussion we make the assumption that the shocks are planar.

III. AFFECT OF SHOCKS ON IMPLODING PLASMA

At the location of the shock a discontinuity will be present in the ablated plasma flow. The velocity component perpendicular to the shock v_\perp will decrease and the density ρ will increase, according to the oblique shock jump conditions¹⁶

$$\frac{v_{\perp sh}}{v_{\perp abl}} = \frac{1}{\eta} = \left(\frac{\rho_{sh}}{\rho_{abl}} \right)^{-1} = \frac{M_\perp^2(\gamma - 1) + 2}{M_\perp^2(\gamma + 1)} \sim 0.14, \quad (1)$$

where the subscripts *abl* and *sh* refer to the preshock (ablation) flow and the post shock flow respectively, $M_\perp = M \sin(\beta) = 3.15$ is the Mach number perpendicular to the shock, the adiabatic index $\gamma = 1.1$ is determined using equations in Ref. 16 and η is defined as the compression ratio across the shock. In addition to these jumps in velocity and density, the temperature of the flow will also be increased.¹⁶

The jump in velocity component perpendicular to the shock results in an effective deflection of the flow away from the inner wire, and the formation of secondary shocks midway between the inner wires (see diagram in Fig. 2). We note that as the inward flow from the outer array approaches the inner array it is azimuthally uniform due to thermal expansion of the streams; the shock structure should be insensitive to the relative azimuthal positions of the outer and inner arrays (the relative *clocking* of the arrays). Also the shock angles and hence jump conditions should be independent of inner wire number.

We will next consider what effect this network of shocks, and the associated jumps in plasma conditions could have on the dynamics of the snowplow piston of the imploding outer array. This outer array will implode in an identical manner to a single array until it reaches the inner array and current is switched out of the piston into the inner wire array. In the vicinity of the inner array the piston experiences shocked prefill material, which has enhanced density, and reduced velocity (Eq. (1)), which in turn increases the difference in velocity Δv between the piston and prefill material. The changes in prefill density and velocity each have the

effect of increasing the rate that energy $\rho(\Delta v)^3$ is absorbed by the piston, and subsequently radiated as snowplow emission. As both the ion-ion mean free path and the ion electron equilibration time are small with respect to the characteristic timescales of the implosion, any power gained by the piston through accretion of material is immediately radiated.¹² Before the piston loses significant momentum it radiates powers exceeding the snowplow emission from the equivalent single array, which is measured as an interaction pulse.

This process can be demonstrated numerically by considering a snowplow model of the implosion of the outer array on MAGPIE. A snowplow model similar to that described by Ref. 14 is adapted to model the implosion of a nested wire array in the presence of the observed shocks. Plasma prefill is defined, according to the rocket model,¹² modified to incorporate the shock jump conditions (e.g., Eq. (1)). To mimic the azimuthal shape of the shock structures, the density and velocity are uniformly ramped to the post-shock values over a distance similar to the inter-wire gap of the inner array.

Results of the model as these conditions are imposed on the piston are shown in Fig. 3. Plots are shown of current (I_{piston}), radial position (R_{piston}), velocity (v_{piston}), along with radiated power ($P \sim \rho(\Delta v)^3$) from the snowplow model for single and nested arrays on MAGPIE. Current is immediately switched out of the piston as the imploding sheath reaches the inner array (see Fig. 3(a)). Immediately after the piston has passed the inner array it starts to experience the modified prefill plasma conditions.

The model predicts that the snowplow emission from a nested array is greater than that from a single array soon after the outer array passes the inner array, as shown in Fig. 3(c). This prediction can be compared to side-on self-emission imaging on MAGPIE shown in Figures 4(a) and 4(b), which are self-emission images taken 10 ns apart as the imploding outer array reaches the inner array. This shot is a similar, but not identical setup to that used in Fig. 2, but is later in the evolution of the system, after the outer array has begun to implode, and is arriving at the inner array. In the XUV

images, strongest emission is seen immediately after each discrete bubble passes the inner array. The data are in agreement that the interaction emission is after the piston has passed the inner, rather than from the inner wires, or from the piston prior to reaching the inner. We note that this experimental data is in contradiction to predictions from other models of interaction emission,^{17,18} which determine that the emission should be from either the actual inner array wires or from the outer array material before it passes the inner wire array.

Another comparison between the model predictions and experimental data can be made by considering the trajectory of the outer array after it passes the inner array, and before the implosion of the inner. In the previous work by Bland *et al.*,⁹ it was determined that, for an identical nested wire array setup, also fielded on MAGPIE, only a negligible fraction of the current measured to pass through the inner array prior to the interaction (<1 kA through the inner array once the outer wire array begins to form a corona). Importantly, Bland *et al.*,⁹ demonstrated these arrays operate in a transparent mode, with inner array wire cores remaining at $\sim 15\text{--}25\ \mu\text{m}$ core sizes, which indicated a transparency of $\sim 98\%$ (determined by the fraction of the surface area at the inner array radius occupied by inner wire cores).

Given that the inner array is transparent,⁹ the only mechanism for the piston to lose momentum is by accreting (and hence accelerating) the snowplowed material; this mechanism is incapable of retarding the piston below the flow velocity of the prefill material. Fig. 3(d) shows that the model estimates that post-interaction the piston is decelerated to a velocity $v_{\text{piston}} \sim 8\ \text{cm}/\mu\text{s}$, as the piston accretes material of a velocity $v_{\text{sh}} \sim 2.1\ \text{cm}/\mu\text{s}$ (Eq. (1)), which is less than the ablation velocity ($v_{\text{abl}} \sim 15\ \text{cm}/\mu\text{s}$). Examining the experimental trajectory in Fig. 4(b) (as measured by radial optical streak) we see that the piston velocity drops to a value $v_{\text{piston}} \sim 7.2\ \text{cm}/\mu\text{s}$. For this piston velocity to drop below the ablation velocity requires that the material it is accreting is traveling at a velocity below the initial ablation velocity.

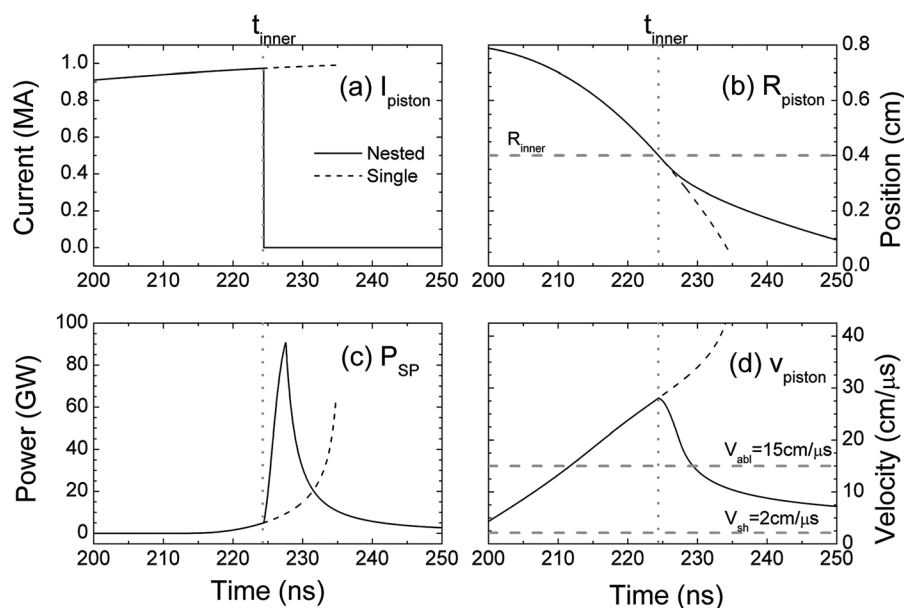


FIG. 3. Snowplow implosion variables for a MAGPIE implosion with (solid lines) and without (dotted lines) an inner array (a) current, (b) radial position, (c) power emitted by the snowplow piston, and (d) piston velocity.

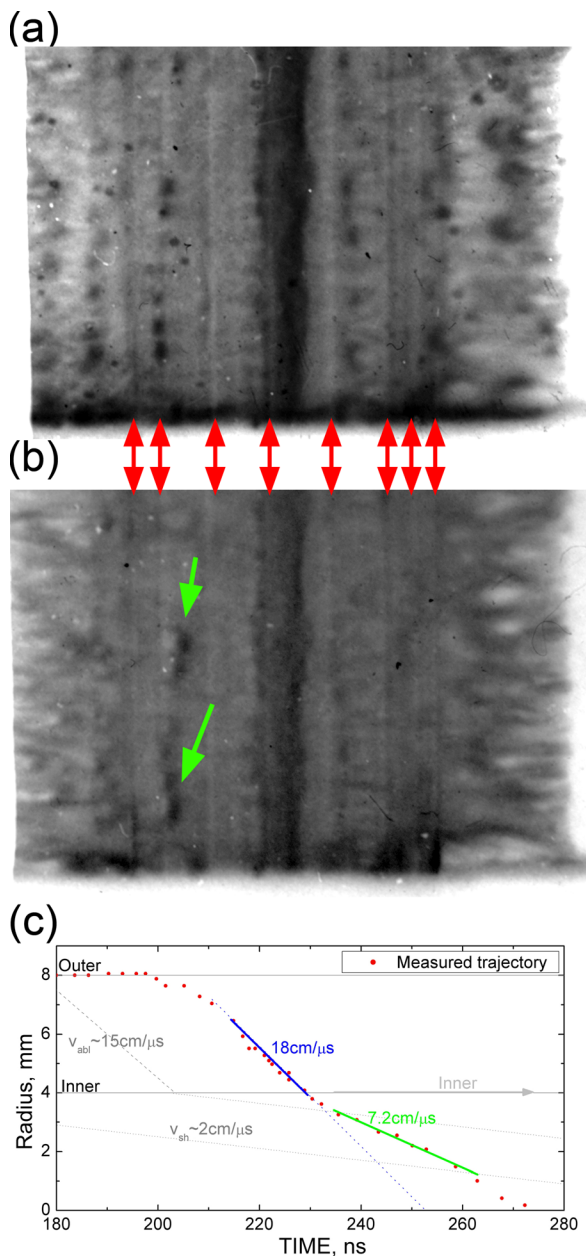


FIG. 4. (a) XUV self-emission ($h\nu > 30 \text{ eV}$) from side-on to a nested Al array at 201 ns, immediately before interaction of the outer with the inner array. (b) XUV self-emission at 211 ns as sections of the imploding outer array pass the inner wire array. The bubbles formed during the implosion of the outer array emit as they pass the inner wires and enter the region of inflowing material perturbed by the presence of the inner array. (c) The trajectory of the outer array measured by optical radial streak shows that the imploding sheath decelerates below the ablation velocity ($v_{abl} \sim 15 \text{ cm}/\mu\text{s}$). Shown as grey dotted lines are assumed trajectories of ablation streams, initially traveling at the ablation velocity, and later at the shocked velocity, as shown in by Eq. (1).

The imploding sheath of a wire array is not a perfectly thin uniform cylinder, instead it has a finite thickness, as well as azimuthal and axial structure.^{12,13} To account for this thickness it would be necessary to smooth the modeled power pulse by a characteristic timescale τ_{smooth} in order to recreate the experimental data. The thickness of the sheath, and in particular the axial and azimuthal variations will depend greatly on the number of wires in the outer array.¹³ For the moderate wire numbers fielded on MAGPIE the

imploding sheath may be sufficiently non-uniform that the temporal smoothing prevents the spatially integrated power diagnostics from resolving the interaction pulse.

The interaction pulse is significantly better defined on the Z generator than MAGPIE, so now that we have indirect evidence for the mechanism responsible from MAGPIE we switch our attention to Z. For Z, the densities of the ablated outer wire material at the location of the inner wires ($5 \text{ kg}/\text{m}^3$) and the velocity of the implosion ($30 \text{ cm}/\mu\text{s}$) as it reaches ablated is much higher than on MAGPIE. In an ideal case, when this implosion meets ablated material that has been shocked, so is traveling at a velocity $< 15 \text{ cm}/\mu\text{s}$, the mechanism described can, in theory, lead to 10 s of terawatts of additional snowplow power (above the snowplow power emitted by a single array). As determining the angles of the shocks on Z, and the effects of opacity are non-trivial, we turn to magnetohydrodynamic (MHD) simulations to determine the powers that can be emitted by this mechanism. We will use MHD simulations to investigate the details of this mechanism on Z.

IV. MHD SIMULATIONS OF INTERACTION PULSE ON Z

The 3-dimensional Gorgon resistive MHD code¹⁷ has previously been utilized to model wire array z-pinch. The interaction and the transfer of current between nested wire arrays have previously been described in simulations by assuming that magnetic flux trapped between the inner and outer arrays is compressed, inducing a current in the inner array which rapidly heats and ablates that material. This implies that ohmic heating of the inner array wires is the dominant heating mechanism for the nested interaction radiation pulse. Here, we simulate a nested array with 2.5 mg, 20 mm diameter outer array and 2.5 mg 12mm diameter inner array on Z in three dimensions using the Gorgon code. These simulations have previously been benchmarked to experimental data from Z,¹⁹ showing good agreement with the transparency of the interaction.

Figure 5(a) shows a breakdown of the energetics of the interaction pulse obtained in these calculations. Viscous heating resulting from the shock interaction of the highly supersonic imploding outer array is seen to dominate, with ohmic heating relegated to the tail of the interaction pulse. If we separate the energetics into the radiated power associated with the inner and outer array materials, we can see this viscous shock heating is almost exclusively associated with just the outer array material (Figure 5(b)). Radiation emitted by the inner array material is seen to rise later in time, consistent with it being the product of the ohmic heating. This demonstrates that the nested interaction pulse is effectively the imploding outer array interacting with its own material. The imploding surface has encountered the density jump created as supersonic ablated precursor plasma was shocked around the stationary inner wires, in the manner similar to that described above. The outer array then transfers its current to the inner, which ohmically heats and ablates, but this mainly contributes to the tail of the interaction pulse.

These simulations have indicated that, for this setup, the interaction pulse is produced by accretion of shocked outer

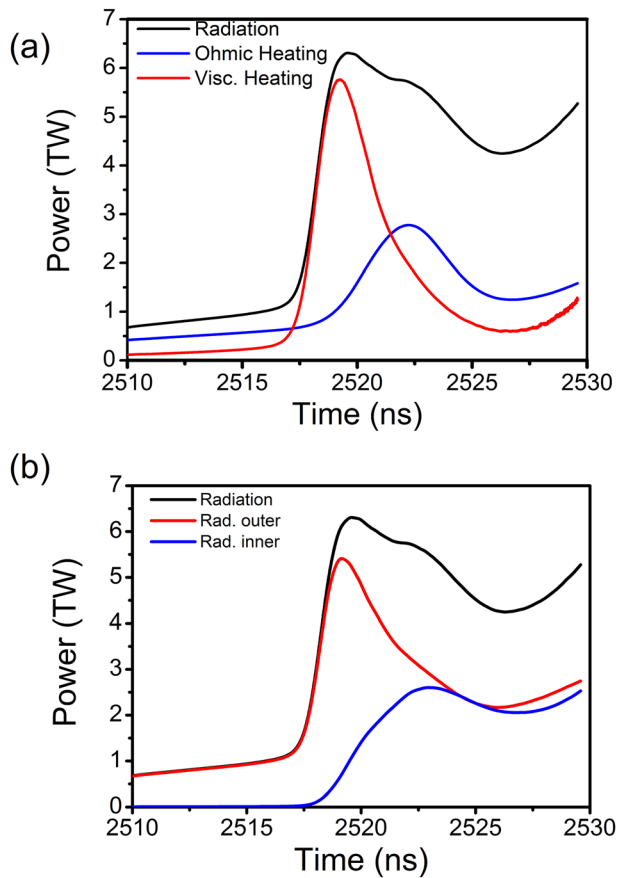


FIG. 5. (a) Contributions of viscous shock heating and ohmic heating to nested interaction pulse. (b) Interaction pulse radiation separated into inner and outer material.

array prefill material by the imploding outer wire array; future simulations could look in more detail at how this changes for vastly different initial setups.

V. CONCLUSION

In summary, we have shown with experiments on the MAGPIE generator that the ablated prefill within a nested array is perturbed by the presence of the inner array. Using estimates of the shock jump conditions as the initial condition for a snowplow implosion model, we have shown that snowplow emission is enhanced as the piston accretes the shocked material, despite traveling current free. Data from MAGPIE are in general agreement with predictions made by the snowplow model. MHD simulations demonstrate that a similar mechanism exists on experiments on the Z generator. Finally we note that, due to the dependence of the estimated interaction pulse on only the nature of the ablated flow from the outer array and the imploding piston, the power in the

interaction pulse is independent of the inner array parameters, which is in agreement with experimental evidence.⁵

ACKNOWLEDGMENTS

Sandia National Laboratories is a multi-program laboratory managed and operated by Sandia Corporation, a wholly owned subsidiary of Lockheed Martin Corporation, for the U.S. Department of Energys National Nuclear Security Administration under Contract No. DE-AC04-94AL85000.

¹C. Deeney, M. R. Douglas, R. B. Spielman, T. J. Nash, D. L. Peterson, P. L'Eplattenier, G. A. Chandler, J. F. Seamen, and K. W. Struve, *Phys. Rev. Lett.* **81**, 4883 (1998).

²M. E. Cuneo, R. A. Vesey, G. R. Bennett, D. B. Sinars, W. A. Stygar, E. M. Waisman, J. L. Porter, P. K. Rambo, I. C. Smith, S. V. Lebedev *et al.*, *Plasma Phys. Control. Fusion* **48**, R1 (2006).

³M. E. Cuneo, R. A. Vesey, D. B. Sinars, J. P. Chittenden, E. M. Waisman, R. W. Lemke, S. V. Lebedev, D. E. Bliss, W. A. Stygar, J. L. Porter *et al.*, *Phys. Rev. Lett.* **95**, 185001 (2005).

⁴R. A. Vesey, M. C. Herrmann, R. W. Lemke, M. P. Desjarlais, M. E. Cuneo, W. A. Stygar, G. R. Bennett, R. B. Campbell, P. J. Christenson, T. A. Mehlhorn *et al.*, *Phys. Plasmas* **14**, 056302 (2007).

⁵M. E. Cuneo, D. B. Sinars, E. M. Waisman, D. E. Bliss, W. A. Stygar, R. A. Vesey, R. W. Lemke, I. C. Smith, P. K. Rambo, J. L. Porter *et al.*, *Phys. Plasmas* **13**, 056318 (2006).

⁶J. Davis, N. A. Gondarenko, and A. L. Velikovich, *Appl. Phys. Lett.* **70**, 170 (1997).

⁷S. V. Lebedev, R. Aliaga-Rossel, S. N. Bland, J. P. Chittenden, A. E. Dangor, M. G. Haines, and M. Zakaullah, *Phys. Rev. Lett.* **84**, 1708 (2000).

⁸T. W. L. Sanford, M. E. Cuneo, D. E. Bliss, C. A. Jennings, R. C. Mock, T. J. Nash, W. A. Stygar, E. M. Waisman, J. P. Chittenden, M. G. Haines *et al.*, *Phys. Plasmas* **14**, 052703 (2007).

⁹S. N. Bland, S. V. Lebedev, J. P. Chittenden, C. Jennings, and M. G. Haines, *Phys. Plasmas* **10**, 1100 (2003).

¹⁰S. N. Bland, D. J. Ampleford, S. C. Bott, S. V. Lebedev, J. B. A. Palmer, S. A. Pikuz, and T. A. Shelkovenko, *Rev. Sci. Instrum.* **75**, 3941 (2004).

¹¹D. J. Ampleford, C. A. Jennings, G. N. Hall, S. V. Lebedev, S. N. Bland, S. C. Bott, F. Suzuki-Vidal, J. B. A. Palmer, J. P. Chittenden, M. E. Cuneo *et al.*, *Phys. Plasmas* **17**, 056315 (2010).

¹²S. V. Lebedev, F. N. Beg, S. N. Bland, J. P. Chittenden, A. E. Dangor, M. G. Haines, K. H. Kwek, S. A. Pikuz, and T. A. Shelkovenko, *Phys. Plasmas* **8**, 3734 (2001).

¹³S. V. Lebedev, D. J. Ampleford, S. N. Bland, S. C. Bott, J. P. Chittenden, J. Goyer, C. Jennings, M. G. Haines, G. N. Hall, D. A. Hammer *et al.*, *Plasma Phys. Control. Fusion* **47**, A91 (2005).

¹⁴D. B. Sinars, M. E. Cuneo, E. P. Yu, S. V. Lebedev, K. R. Cochrane, B. Jones, J. J. Macfarlane, T. A. Mehlhorn, J. L. Porter, and D. F. Wenger, *Phys. Plasmas* **13**, 042704 (2006).

¹⁵S. V. Lebedev, F. N. Beg, S. N. Bland, J. P. Chittenden, A. E. Dangor, M. G. Haines, S. A. Pikuz, and T. A. Shelkovenko, *Laser Part. Beams* **19**, 355 (2001).

¹⁶R. P. Drake, L. Davison, and Y. Horie, *High-Energy-Density Physics: Fundamentals, Inertial Fusion, and Experimental Astrophysics* (Springer, 2006), pp. 81–85.

¹⁷J. P. Chittenden, S. V. Lebedev, S. N. Bland, A. Ciardi, and M. G. Haines, *Phys. Plasmas* **8**, 675 (2001).

¹⁸R. W. Lemke, J. E. Bailey, G. A. Chandler, T. J. Nash, S. A. Slutz, and T. A. Mehlhorn, *Phys. Plasmas* **12**, 012703 (2005).

¹⁹C. A. Jennings, *Bull. Am. Phys. Soc.* **54**, 135 (2009). Available at <http://meetings.aps.org/link/BAPS.2009.DPP.JI2.4>.